Article

Analyzing and Simulating the Influence of a Water Conveyance Project on Land Use Conditions in the Tarim River Region

Jinyao Lin * and Qitong Chen

School of Geography and Remote Sensing, Guangzhou University, Guangzhou 510006, China
* Correspondence: ljy2012@gzhu.edu.cn

Abstract: Arid and semi-arid areas are facing severe land degradation and desertification due to water scarcity. To alleviate these environmental issues, the Chinese government has launched a "water conveyance" project for environmental protection along the Tarim River. While previous studies have mainly focused on environmental conditions, the influence of these policies on land use conditions remains less explored. Therefore, this study first simulated the land use and land cover (LULC) changes in a major city (Korla) around the Tarim River. We found that the water conveyance routes have exerted notable influences on surrounding LULC changes. Next, we primarily focused on the LULC changes among different reaches of the Tarim River. We found that water and forest areas in the lower reaches have increased at the expense of a slight decrease in such areas in the upper and middle reaches, which suggests that the water conveyance policy may also have unintended consequences. These findings could attract the attention of decision makers in many other arid and semi-arid areas, and they could provide practical policy implications for other similar inter-basin water conveyance projects. The benefits and risks of these man-made projects should be carefully balanced.

Keywords: cellular automata; water conveyance; land use and land cover; geosimulation; Xinjiang

1. Introduction

Land use and land cover (LULC) change is a primary issue in global environmental change and sustainable development [1–5]. Land use activities will inevitably have significant influences on the planet's land surface [6–9]. Numerous environmental and social issues are associated with rapid urbanization and population growth throughout the world [10–13]. In particular, arid and semi-arid areas suffer from a series of environmental problems, such as land degradation [14–16], desertification [17–19], and water scarcity [20–22], even though the urban growth rates are not as high as those in fast-growing regions. It is increasingly important to analyze and simulate the LULC changes in these areas, which can provide practical instructions for environmental management and decision making [23–29].

In arid and semi-arid areas, water resources play fundamental roles in land use and economic development [30–32]. To restrict or stop the flow of water and underground streams for personal use, local residents generally construct a number of dams and ditches along rivers throughout the world. Reservoirs created by dams can not only prevent floods but also provide a large amount of water for various daily activities, such as agricultural irrigation, industrial use, and human consumption [33–35]. However, due to excessive and inefficient water consumption in the upper and middle reaches of some endorheic rivers, the lower reaches are easily affected by water scarcity, especially in drought years [36–38]. To address these problems, some decision makers have decided to convey water resources from the upper to lower reaches [39–42]. Notably, the Chinese government has launched a long-term project called "ecological water conveyance", which aims to protect the environment and natural resources in the lower reaches of the Tarim River Basin, Xinjiang [43–46].

These projects will inevitably affect the surrounding natural environment and ecosystem services. Although a number of studies have analyzed the consequences of such water conveyance projects, two major limitations remain to be explored. First, most previous studies have mainly focused on the influence of water conveyance on environmental conditions. For example, Akron et al. [47] pointed out that water conveyance can restore water flow and enhance ecosystem services in Ayun, Israel; Genereux et al. [48] analyzed the advantages of water conveyance in the lowland rainforest of Costa Rica; Zhao et al. [49] demonstrated that such projects are able to restore biodiversity and vegetation in the lower reaches of the Tarim River; and Guo et al. [50] found that water conveyance has raised the groundwater level in the lower reaches of the Heihe River Basin, China. However, less attention has been given to the effects of these man-made policies on land use conditions [51,52].

Second, it is not easy to identify the influences of water conveyance on land use conditions simply based on remote sensing monitoring due to the complexity of LULC changes. Interestingly, LULC models (e.g., cellular automata) have the potential to address this matter by simulating whole change processes. For example, Mubako et al. [53] evaluated past and future LULC changes in the semi-arid Dodoma, Tanzania, by combining artificial neural networks and CA models. Hou et al. [54] simulated LULC changes in the Tarim River Basin with the support of the CA–Markov model, and the results revealed the spatiotemporal pattern of land use in the future. Mamitimin et al. [55] analyzed the spatiotemporal LULC change in Urumqi, Xinjiang, during 1980–2020, and then projected future LULC change in 2050 under several scenarios by using a CA model. Xie et al. [56] utilized a LULC model to simulate the LULC changes and ecosystem service values in the arid Aksu River Basin. Alqadhi et al. [57] investigated the LULC changes in a semi-arid region of Saudi Arabia from 1990 to 2018, and they further simulated the LULC changes in 2040 by using the multilayer perceptron neural network land change model. All these previous studies have provided important insights into LULC change modeling in arid and semi-arid areas. Nevertheless, the influences of water conveyance have rarely been considered in LULC change simulation and prediction. Since the implementation of water conveyance projects could have a considerable influence on LULC changes, a meaningful attempt should be made to carefully consider the influences of water conveyance on LULC change simulation and prediction. Therefore, the aim of this study is to fill these gaps by addressing the following two research questions: (1) What are the positive and negative effects of man-made water conveyance policies on land use conditions in arid and semi-arid areas? (2) Can the consideration of the influences of water conveyance improve the accuracies of LULC change modeling?

2. Materials and Methods

2.1. Study Area and Spatial Data

The Xinjiang Uyghur Autonomous Region is situated in northwestern China. As shown in Figure 1, this region is the largest Chinese administrative division, with a total land area of more than 1.66 million km^2. Due to the extremely low precipitation and intensive evaporation in this area, most of the rivers in Xinjiang are fed by the snowmelt of the surrounding mountain ranges [33,58]. As a result of excessive and inefficient water consumption in the upper and middle reaches, many rivers and lakes have begun to dry up, dating back to the 1970s. Specifically, the Tarim River region, which is located in the central part of Xinjiang, has witnessed a substantial decrease in riparian vegetation (e.g., *Populus euphratica*) and wildlife.
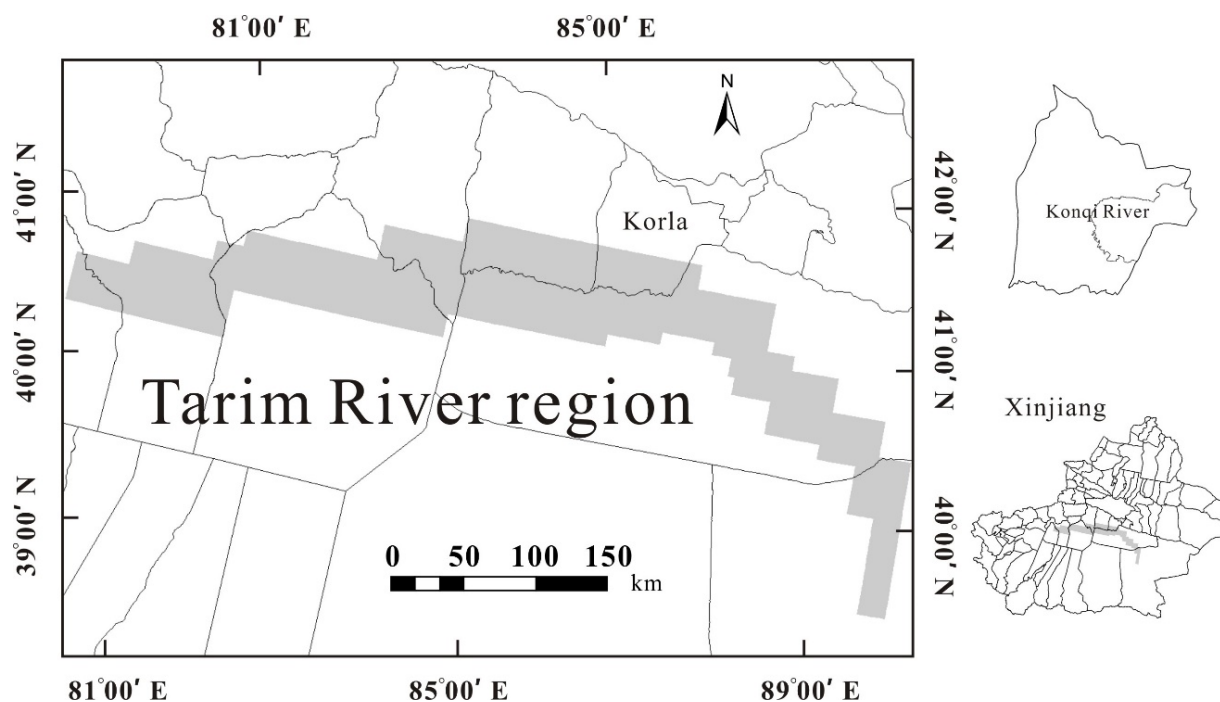
Figure 1. Location of the study area.

The Tarim River, which is the largest endorheic river in China, originates from the union of the Aksu River, Yarkand River, and Hotan River. The Tarim River flows in an eastward direction around the Taklamakan Desert [59]. To protect the natural environment and resources, the Chinese government has launched well-known "ecological water conveyance" projects. From 14 May to 12 July 2000, 98 million cubic meters of water was conveyed to the lower reaches of the Tarim River. Since then, such water conveyance efforts have been made annually. Now, the water can finally flow into the tail section (Taitema Lake) in most cases.

To systematically investigate the influence of LULC on water conveyance, this study obtained time series remote sensing classification data from 1990, 2000, 2010, and 2020. The data were generated by manually interpreting the Landsat remote sensing images with a spatial resolution of 30 m. A classification scheme of two levels, with level-1 including six major classes and level-2 including more specific classes, was adopted. As listed in Table 1, the level-1 classification consists of farmland, forest, grassland, water area, built-up area, and unused land. The results were further classified into sub-categories of level-2.

Specifically, the widely used random forest algorithm was applied to the timeseries Landsat remote sensing images for supervised classification. In our research, both the training and testing samples for LULC classification were obtained from the remote sensing images using the China multi-period land use and land cover (CNLUCC) data from the Chinese Academy of Sciences and high-resolution Google Earth Pro images as reference sources. Firstly, all of the samples (5000 samples for each year) were selected from the CNLUCC data according to a stratified random sampling method. Secondly, we carefully corrected the misclassified samples with the support of Google Earth Pro images. Thirdly, the corrected samples were randomly classified as training (80%) and testing sub-datasets (20%). Finally, the LULC datasets from 1990, 2000, 2010, and 2020 could be obtained based on the above methodological framework. The performance of the remote sensing classification was validated according to the overall accuracies. The overall accuracies of the LULC datasets from 1990, 2000, 2010, and 2020 were found to be 92.6%, 94.7%, 92.2%, and 95.1%, respectively. The above results demonstrate that the classified LULC datasets have high reliability, which can be further utilized for LULC change assessment, simulation, and prediction.

Table 1. Land use and land cover classification scheme.

Level-1 Classification	Level-2 Classification	Level-1 Classification	Level-2 Classification
Farmland	Paddy field Dryland farming	Built-up area	Urban land Rural settlement
Forest	Dense forest		Other built-up area
	Shrubland Sparse forest Other forest	Unused land	Desert Gobi Saline-alkali soil
Grassland	Dense grassland Moderate grassland Sparse grassland		Swampland Bare soil Bare rock
Water area	River		Other unused land
	Lake Reservoir and pond Snow cover Bottomland	–	–

2.2. Land Use and Land Cover Change Monitoring

Timeseries remote sensing classification data are useful for analyzing LULC changes over a long period. We adopted the commonly used land use conversion matrix for LULC change monitoring in the study area. According to previous studies, the annual change rate for each LULC category over different periods can be directly compared by using the following formula:

$$R = \frac{L_b - L_a}{L_a} \times \frac{1}{T} \tag{1}$$

where R is the rate of LULC changes during a specific period, L_a and L_b are the total area of a single LULC category at the beginning and the end of this period, and T is the length of this period (e.g., in years).

2.3. Land Use and Land Cover Change Modeling

Since this study involves six level-1 LULC categories, we selected the artificial neural network cellular automaton (ANN-CA) model to simulate the spatiotemporal LULC changes in the study area. Many studies have demonstrated that the ANN-CA model is a successful tool for modeling multiple LULC changes [60–62].

An ANN contains three different layers: an input layer, hidden layer, and output layer. The input layer includes m neurons, which are used to receive m different spatial factors associated with LULC changes. In the hidden layer, the number of neurons is generally set as $2m/3$, while the number of neurons in the output layer is the same as the number of LULC categories. Each output neuron represents a change probability corresponding to a single LULC category. We trained the ANN by using the commonly used back propagation learning model. More details are presented as follows:

First, a two-dimensional matrix will be used to stand for a study area. Each matrix entry is equipped with m attribute values corresponding to m spatial factors. These values, which will be input into the first layer of the ANN, can be represented as follows:

$$X(k,t) = [x_1(k,t), x_2(k,t), \ldots, x_m(k,t)]^{\mathrm{T}} \tag{2}$$

where $x_i(k,t)$ denotes the ith attribute value of cell k at time t, and T refers to the transpose of a matrix.

Second, these attribute values will be further transferred to the hidden layer by using the following formula [61]:

$$net_j(k,t) = \sum_i w_{i,j} x_i(k,t) \tag{3}$$

where $net_j(k,t)$ denotes the value transferred from cell k at time t to the jth neuron in the hidden layer, and $w_{i,j}$ denotes the weight between the input layer and hidden layer. Then, the hidden layer will respond by using the following sigmoidal function:

$$\frac{1}{1 + e^{-net_j(k,t)}} \tag{4}$$

Third, the response result will be transferred to the output layer as the LULC change probability:

$$p(k,t,l) = \sum_j w_{j,l} \frac{1}{1 + e^{-net_j(k,t)}} \tag{5}$$

where $p(k,t,l)$ denotes the LULC change probability from the current LULC category to a new category l for cell k at time t, and $w_{j,l}$ denotes the weight between the hidden layer and output layer.

In addition, we should also consider a random perturbation factor in accordance with previous studies [63–65]. As a consequence, the LULC change probability can be formulated as follows:

$$p(k,t,l) = \sum_j w_{j,l} \frac{1}{1 + e^{-net_j(k,t)}} \times \left(1 + (-\ln\gamma)^\alpha\right) \tag{6}$$

where γ denotes a stochastic number within the range [0, 1], and α is a parameter for determining the stochastic degree.

Each land use cell can only be converted to a single LULC category at a time. Therefore, only the maximum change probability will be considered. We used a threshold value within the range [0, 1] to ensure that the land use cells changed step by step. This procedure can be formulated by using the following equation:

$$S_k^{t+1} = \begin{cases} q, & \max[p(k,t,l)] > p_{\text{threshold}} \\ S_k^t, & \max[p(k,t,l)] \leq p_{\text{threshold}} \end{cases} \tag{7}$$

where S_k^t is the LULC category for cell k at time t, S_k^{t+1} is the LULC category for cell k at time $(t + 1)$, q denotes the LULC category with the maximum change probability, and $p_{\text{threshold}}$ denotes a threshold value determined by the total number of land use cells derived from the last remote sensing classification data.

Finally, we used the figure of merit (FoM) and confusion matrix to measure the performance of different simulation results given that the other metrics affected by large numbers of persistence grid cells (e.g., kappa) are potentially misleading. The FoM, the ratio of the intersection of observed changes and simulated changes to the union of observed changes and simulated changes is, therefore, a more suitable metric for evaluating LULC modeling [66]. The FoM can be calculated as follows:

$$\text{FoM} = \text{Hits}/(\text{Hits} + \text{Misses} + \text{False alarms} + \text{Wrong gaining category}) \tag{8}$$

where Hits refers to the correctness produced by observed change simulated as change, Misses refers to the mistake caused by observed change simulated as persistence, False alarms refers to the mistake caused by observed persistence simulated as change, and Wrong gaining category refers to the mistake caused by observed change simulated as the wrong gaining category.

Generally speaking, three years (e.g., Year 1, Year 2, and Year 3) of LULC datasets are necessary for the validation of LULC change modeling. More specifically, the LULC datasets in Year 1 and Year 2 are employed to calibrate the LULC change model, while the LULC datasets in Year 2 and Year 3 are employed to validate the generalization ability of the above calibrated LULC change model. To this end, firstly, the LULC change model in our research was calibrated according to the samples of LULC changes between 1990 and 2000. Secondly, we simulated the LULC changes during this period based on the calibrated

LULC change model and compared the simulation result with the actual remote sensing classification data in 2000. This comparison can assess the performance of the above model calibration procedure. Thirdly, we further predicted the LULC changes between 2000 and 2010 with the support of this well-calibrated LULC change model. The prediction result was compared with the actual remote sensing classification data in 2010, which can adequately validate the generalization ability of the above calibrated LULC change model.

3. Implementation and Results

In this study, we first simulated the LULC changes in a city around the Tarim River to identify the influence of the water conveyance project. Next, we primarily focused on the comparison of LULC changes among the upper, middle, and lower reaches of the Tarim River region. More detailed results are presented in the following subsections.

3.1. Modeling Land use and Land Cover Changes in Korla Using ANN-CA

Korla, the largest city in southern Xinjiang that has benefited from the ecological water conveyance project, was selected for LULC change modeling. We only considered the level-1 classification results in this attempt. Two experiments were carried out to identify the influence of water conveyance routes by using the effective ANN-CA model. Based on previous studies, we first simulated the LULC changes from 1990 to 2010 by considering various relevant spatial factors [67–72]. As listed in Table 2, the only difference between the first and second experiments is that the latter also considers the location of the water conveyance routes (i.e., the Konqi River).

Table 2. Spatial factors used for modeling land use and land cover changes.

Spatial Factor	Acquisition Method
Distance from a cell to the nearest country center Distance from a cell to the nearest city road Distance from a cell to the nearest country road Distance from a cell to the nearest water body ***Distance from a cell to the Konqi River (DisKonqi)***	Euclidean Distance function in ArcMap
Slope	Digital Elevation Model
Area of farmland within a cell's 3 × 3 neighborhood Area of forest within a cell's 3 × 3 neighborhood Area of grassland within a cell's 3 × 3 neighborhood Area of water area within a cell's 3 × 3 neighborhood Area of built-up area within a cell's 3 × 3 neighborhood Area of unused land within a cell's 3 × 3 neighborhood	Focal Statistics function in ArcMap
Current LULC category	LULC classification data

In this study, the input layer of the ANN included twelve/thirteen neurons that represented the spatial factors mentioned above, while the hidden layer had eight neurons. Six neurons were needed in the output layer to represent six level-1 LULC categories. Each output neuron offered a conversion probability corresponding to one category. We randomly selected twenty percent of the samples from the remote sensing classification data, among which fifteen percent were used for training and five percent for testing. A cell's various spatial attributes (given in Table 2) and its final LULC category were regarded as independent and dependent variables, respectively [73]. We built the ANN-CA model with the support of the MATLAB platform.

Firstly, we simulated the spatiotemporal LULC changes in Korla from 1990 to 2000. The simulation result was compared with the actual remote sensing classification data to assess the performance of the two experiments (see Figure 2). As shown in Table 3, we adopted the figure of merit (FoM) and confusion matrix to measure the simulation accuracies. We found that there was only a marginal difference between the accuracy values,

which means that the "distance from a cell to the Konqi River" was not that influential before the implementation of the conveyance project.
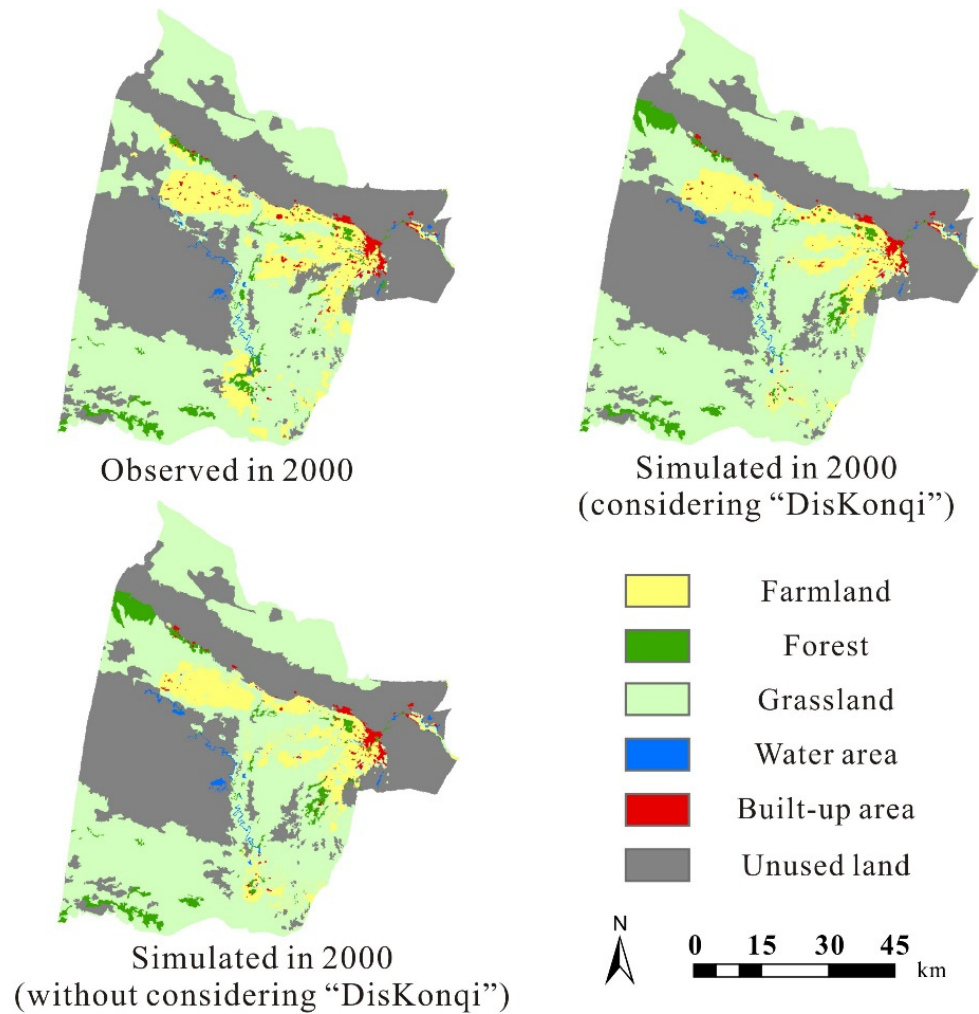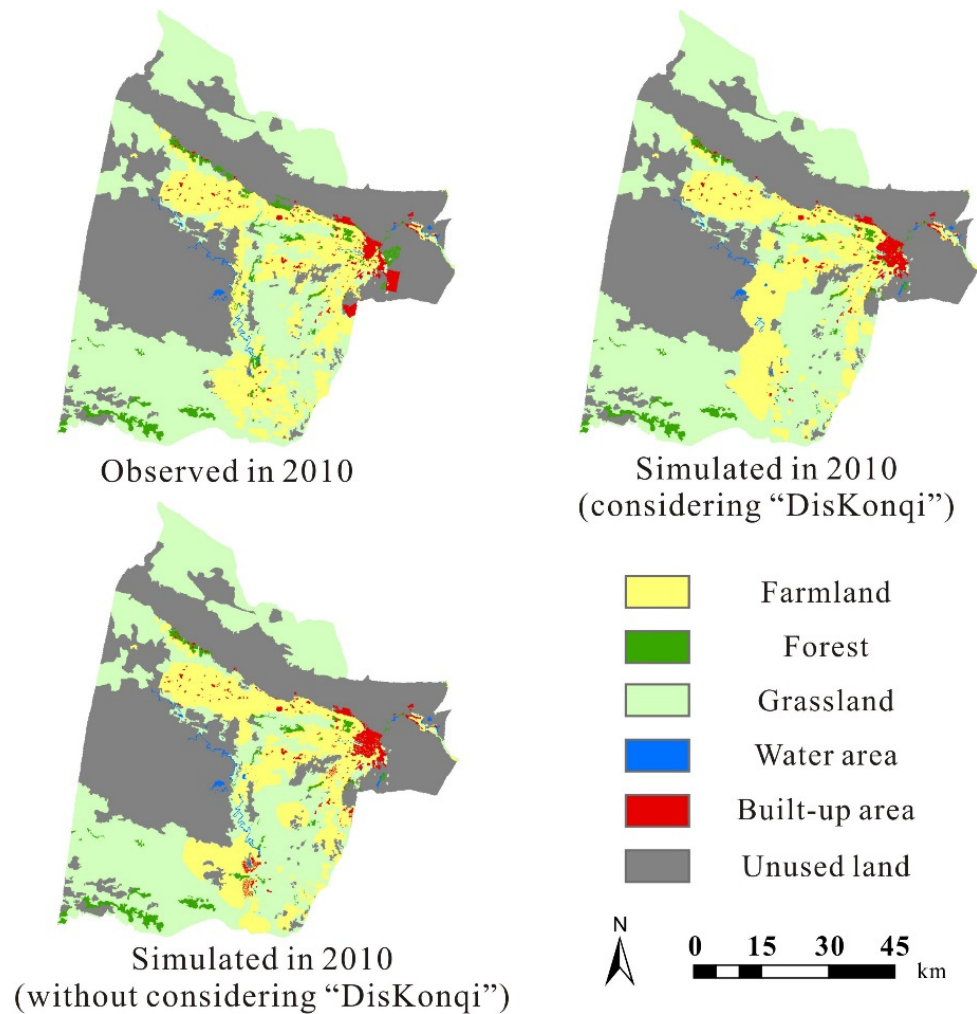

Figure 2. Two simulation results of LULC changes in Korla from 1990 to 2000.

Table 3. Confusion matrix for modeling LULC changes in Korla from 1990 to 2000 (in km^2).

Observed in 2000		Farmland	Forest	Grassland	Water	Built-Up	Unused
	Farmland	17.65	0.31	3.43	0.01	0.60	0.19
	Forest	0.15	4.27	3.48	0.01	0.02	0.04
Simulated	Grassland	11.28	1.71	113.43	0.06	0.26	10.54
in 2000 (without	Water	0.02	0.01	0.14	0.96	0.01	0.37
considering "*DisKonqi*")	Built-up	0.15	0.02	0.04	0.00	1.90	0.12
	Unused	0.67	0.16	4.89	0.18	0.10	110.90
	FoM	0.075		Overall accuracy		86.47%	
	Farmland	19.26	0.36	2.54	0.01	0.49	0.19
	Forest	0.13	4.40	3.46	0.01	0.02	0.04
Simulated	Grassland	9.74	1.53	114.35	0.06	0.11	10.56
in 2000 (considering	Water	0.01	0.01	0.12	0.96	0.00	0.37
"*DisKonqi*")	Built-up	0.12	0.02	0.05	0.00	2.16	0.12
	Unused	0.66	0.16	4.89	0.18	0.11	110.89
	FoM	0.081		Overall accuracy		87.48%	

　　　Secondly, we simulated the LULC changes in Korla from 2000 to 2010. The results are displayed in Figure 3 and Table 4. The simulation result is much closer to the actual remote

sensing classification data if the locations of the water conveyance routes are taken into consideration. For example, although the two overall accuracies are similar, the values of the FoM, which focuses on the changed parts rather than all the land use cells, are quite different (0.177 and 0.228). In addition, we found that most LULC changes occurred around the Konqi River, according to the visual comparison. These experiments demonstrate that the water conveyance route has been an important factor for LULC changes after the implementation of the conveyance project.

Figure 3. Two simulation results of LULC changes in Korla from 2000 to 2010.

3.2. Comparing LULC Changes in the Xinjiang and Tarim River Regions

To systematically investigate the influences of water conveyance projects on land use conditions, we further compared the spatiotemporal LULC changes in the whole Xinjiang area and the Tarim River region from 1990 to 2020. The results are summarized in Tables S1 and S2 (Supplementary Materials). For Xinjiang, the LULC change patterns during these three ten-year periods were quite similar. Generally, the areas of farmland and built-up land continuously increased. In addition, forest and water areas increased during 1990–2000 and remained steady afterwards. For the Tarim River region, the area of farmland exhibited a much higher annual growth rate. Forest and water areas also expanded dramatically at first, but then began to decrease after 2000. These results indicate that the LULC changes in the Tarim River region are substantially different from those in Xinjiang, even though the Tarim River region is a major part of this province.

Table 4. Confusion matrix for modeling LULC changes in Korla from 2000 to 2010 (in km^2).

Observed in 2010		Farmland	Forest	Grassland	Water	Built-Up	Unused
	Farmland	34.11	0.59	10.20	0.00	0.03	0.11
	Forest	0.28	4.88	0.00	0.00	0.00	0.00
Simulated	Grassland	9.65	0.03	100.44	0.00	0.02	0.00
in 2010 (without	Water	0.01	0.00	0.00	1.15	0.00	0.05
considering "*DisKonqi*")	Built-up	1.15	0.11	0.05	0.00	2.96	0.00
	Unused	1.25	1.20	0.02	0.00	1.04	118.76
	FoM	0.177		Overall accuracy		91.04%	
	Farmland	35.64	0.56	6.36	0.29	0.09	2.65
	Forest	0.12	5.03	0.00	0.00	0.00	0.00
Simulated	Grassland	9.21	0.02	104.34	0.01	0.05	0.00
in 2010 (considering	Water	0.01	0.00	0.01	0.86	0.00	0.05
"*DisKonqi*")	Built-up	0.75	0.01	0.01	0.00	2.89	0.03
	Unused	0.73	1.19	0.00	0.00	1.02	116.18
	FoM	0.228		Overall accuracy		91.96%	

To further explore the LULC changes in the Tarim River region, we made a comparison among its upper, middle, and lower reaches during the above three periods. The results are summarized in Tables 5–7 and Figures 4–6. We found that these three sub-regions shared similar LULC change patterns at first (1990–2000). For example, the areas of farmland, forest, and water exhibited an obvious upward trend at the expense of grassland areas. However, there were enormous differences after the implementation of the ecological water conveyance project in 2000. Water and forest areas began to decrease in the upper and middle reaches, while they substantially increased in the lower reaches from 2000 to 2010. Most of these increases were in lakes in the tail section (Taitema Lake) and in dense forests, according to the level-2 classification results. In addition, water areas in the upper and middle reaches continued to shrink during 2010–2020. Furthermore, the annual growth rate of farmland areas has also slowed. However, the water areas in the lower reaches have remained relatively stable.

Table 5. Land use and land cover changes in the upper reaches of the Tarim River (in km^2).

2000 \ 1990	Farmland	Forest	Grassland	Water	Built-Up	Unused	Total
Farmland	1197.00	14.85	341.95	3.55	12.45	95.74	1665.52
Forest	25.89	1631.41	1123.96	19.35	1.37	251.36	3053.34
Grassland	15.47	93.35	6595.33	23.91	5.94	208.32	6942.32
Water	9.59	26.70	140.99	549.31	0.15	8.94	735.69
Built-up	11.28	0.12	4.46	0.02	25.70	0.20	41.77
Unused	20.12	35.69	726.18	36.94	0.79	4808.08	5627.79
Total	1279.34	1802.11	8932.87	633.07	46.40	5372.65	
R	6.04%	13.89%	−4.46%	3.24%	−1.99%	0.95%	

2010 \ 2000	Farmland	Forest	Grassland	Water	Built-Up	Unused	Total
Farmland	1654.06	263.76	295.87	15.51	0.17	91.13	2320.49
Forest	0.00	2767.99	3.07	0.21	0.00	15.79	2787.06
Grassland	3.65	15.15	6635.55	77.81	0.00	41.34	6773.50
Water	0.00	3.68	5.67	639.97	0.00	15.56	664.90
Built-up	7.81	0.00	1.06	0.00	41.60	0.01	50.48
Unused	0.00	2.75	1.10	2.20	0.00	5463.96	5470.01
Total	1665.52	3053.34	6942.32	735.69	41.77	5627.79	
R	7.87%	−1.74%	−0.49%	−1.92%	4.17%	−0.56%	

Table 5. *Cont.*

2020 \ 2010	Farmland	Forest	Grassland	Water	Built-Up	Unused	Total
Farmland	2256.75	110.02	93.98	16.63	1.59	29.38	2508.34
Forest	14.95	2625.40	19.97	3.07	0.25	16.62	2680.26
Grassland	42.43	37.05	6595.90	34.94	0.10	11.36	6721.79
Water	2.03	4.70	3.68	597.08	0.04	2.24	609.76
Built-up	2.80	0.05	0.41	0.01	48.49	0.03	51.79
Unused	1.54	9.86	59.56	13.16	0.03	5410.37	5494.51
Total	2320.49	2787.06	6773.50	664.90	50.48	5470.01	
R	1.62%	−0.77%	−0.15%	−1.66%	0.52%	0.09%	

Table 6. Land use and land cover changes in the middle reaches of the Tarim River (in km^2).

2000 \ 1990	Farmland	Forest	Grassland	Water	Built-Up	Unused	Total
Farmland	237.85	7.13	177.65	0.47	0.29	15.76	439.15
Forest	1.49	839.78	514.42	14.81	0.05	97.14	1467.69
Grassland	79.35	130.94	6504.48	18.49	0.18	333.54	7066.98
Water	0.04	17.66	35.34	60.01	0.01	8.02	121.08
Built-up	0.87	0.06	0.02	0.00	9.07	0.00	10.02
Unused	0.17	25.39	1004.17	10.46	0.00	2012.55	3052.74
Total	319.77	1020.95	8236.07	104.25	9.60	2467.02	
R	7.47%	8.75%	−2.84%	3.23%	0.88%	4.75%	

2010 \ 2000	Farmland	Forest	Grassland	Water	Built-Up	Unused	Total
Farmland	439.07	39.80	277.33	0.01	0.00	26.31	782.52
Forest	0.00	1427.89	0.01	0.00	0.00	0.00	1427.90
Grassland	0.09	0.00	6789.64	1.21	0.00	0.00	6790.94
Water	0.00	0.00	0.00	119.85	0.00	0.00	119.85
Built-up	0.00	0.00	0.00	0.00	10.02	0.00	10.02
Unused	0.00	0.00	0.00	0.00	0.00	3026.43	3026.43
Total	439.15	1467.69	7066.98	121.08	10.02	3052.74	
R	15.64%	−0.54%	−0.78%	−0.20%	0.00%	−0.17%	

2020 \ 2010	Farmland	Forest	Grassland	Water	Built-Up	Unused	Total
Farmland	768.33	8.24	50.62	0.87	0.39	5.97	834.42
Forest	1.38	1390.31	12.63	2.16	0.06	5.79	1412.34
Grassland	8.27	21.63	6709.66	6.76	0.00	17.03	6763.35
Water	0.48	2.28	2.53	100.85	0.00	1.17	107.31
Built-up	0.37	0.05	0.05	0.01	9.57	0.00	10.06
Unused	3.69	5.39	15.46	9.20	0.00	2996.47	3030.20
Total	782.52	1427.90	6790.94	119.85	10.02	3026.43	
R	1.33%	−0.22%	−0.08%	−2.09%	0.07%	0.02%	

Table 7. Land use and land cover changes in the lower reaches of the Tarim River (in km^2).

2000 \ 1990	Farmland	Forest	Grassland	Water	Built-Up	Unused	Total
Farmland	293.45	9.47	56.06	0.39	7.75	4.11	371.23
Forest	9.48	317.00	209.11	0.25	0.36	22.60	558.80
Grassland	25.16	52.96	3831.37	3.40	0.82	104.39	4018.09
Water	0.28	5.22	51.24	70.05	0.01	12.30	139.10
Built-up	2.83	0.05	0.44	0.01	16.46	0.13	19.92
Unused	3.56	15.82	377.10	10.41	0.09	5204.98	5611.96
Total	334.75	400.53	4525.31	84.50	25.49	5348.50	
R	2.18%	7.90%	−2.24%	12.92%	−4.37%	0.99%	

Table 7. *Cont.*

2010 \ 2000	Farmland	Forest	Grassland	Water	Built-Up	Unused	Total
Farmland	371.19	0.00	25.06	0.68	0.00	0.47	397.40
Forest	0.00	557.76	3.66	0.00	0.00	22.96	584.38
Grassland	0.00	0.73	3969.62	0.00	0.00	7.13	3977.48
Water	0.04	0.30	19.74	138.42	0.00	37.56	196.05
Built-up	0.00	0.00	0.00	0.00	19.92	0.00	19.92
Unused	0.00	0.00	0.00	0.00	0.00	5543.85	5543.85
Total	371.23	558.80	4018.09	139.10	19.92	5611.96	
R	1.41%	0.92%	−0.20%	8.19%	0.00%	−0.24%	

2020 \ 2010	Farmland	Forest	Grassland	Water	Built-Up	Unused	Total
Farmland	390.42	1.32	9.48	0.12	0.74	1.09	403.18
Forest	0.68	565.32	12.26	1.50	0.04	4.22	584.03
Grassland	4.98	12.45	3931.65	1.62	0.12	51.77	4002.58
Water	0.11	1.56	1.04	191.53	0.01	1.34	195.58
Built-up	0.80	0.03	0.14	0.00	19.01	0.00	19.98
Unused	0.41	3.69	22.92	1.28	0.01	5485.43	5513.74
Total	397.40	584.38	3977.48	196.05	19.92	5543.85	
R	0.29%	−0.01%	0.13%	−0.05%	0.06%	−0.11%	
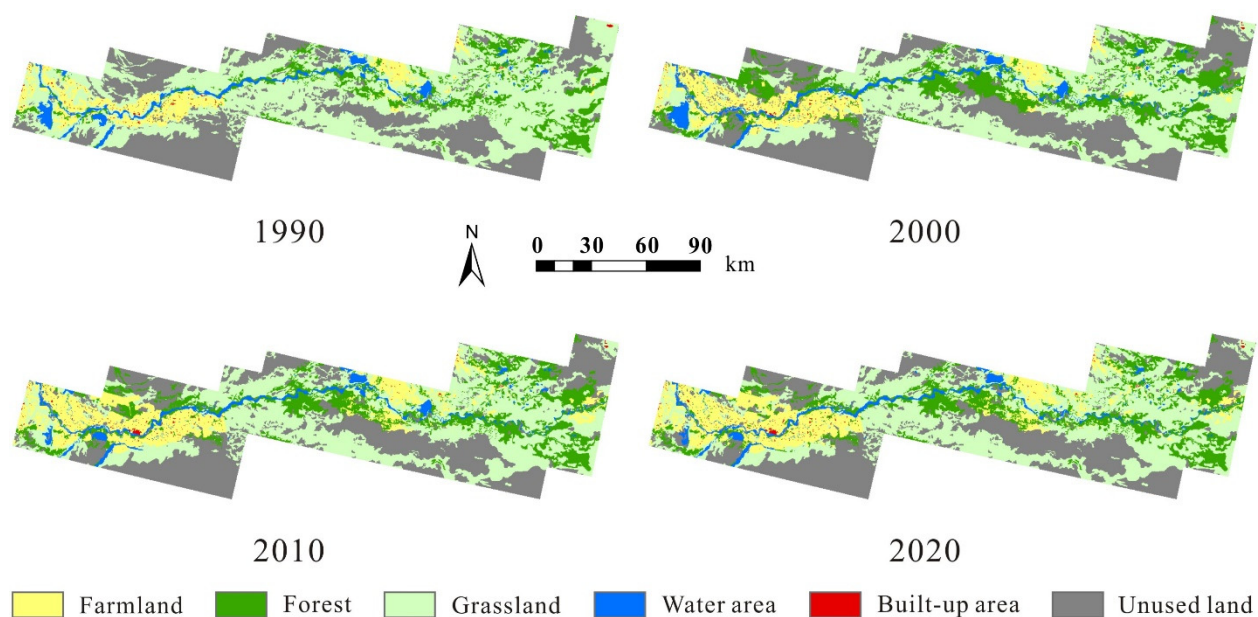
Figure 4. Land use and land cover maps in the upper reaches of the Tarim River.

These phenomena may be largely attributed to the implementation of the ecological water conveyance project. A number of dams, reservoirs, and ditches in the upper and middle reaches of the Tarim River unreasonably restricted and stopped the water flow before 2000. Owing to the abundant water resources, a large quantity of grassland has been changed to farmland and forest. It seems that the water areas in the lower reaches have also increased at a higher rate. However, we found that this observation can be mostly attributed to the expansion of two reservoirs (Qiala and Daxihaizi), according to the level-2 classification results. As increasing amounts of water resources were conveyed to the lower reaches after 2000, much natural vegetation in the upper and middle reaches began to decrease. Nevertheless, the areas of farmland continued to expand to satisfy the food supply due to rapid population growth. This phenomenon further increased the demand for water resources.
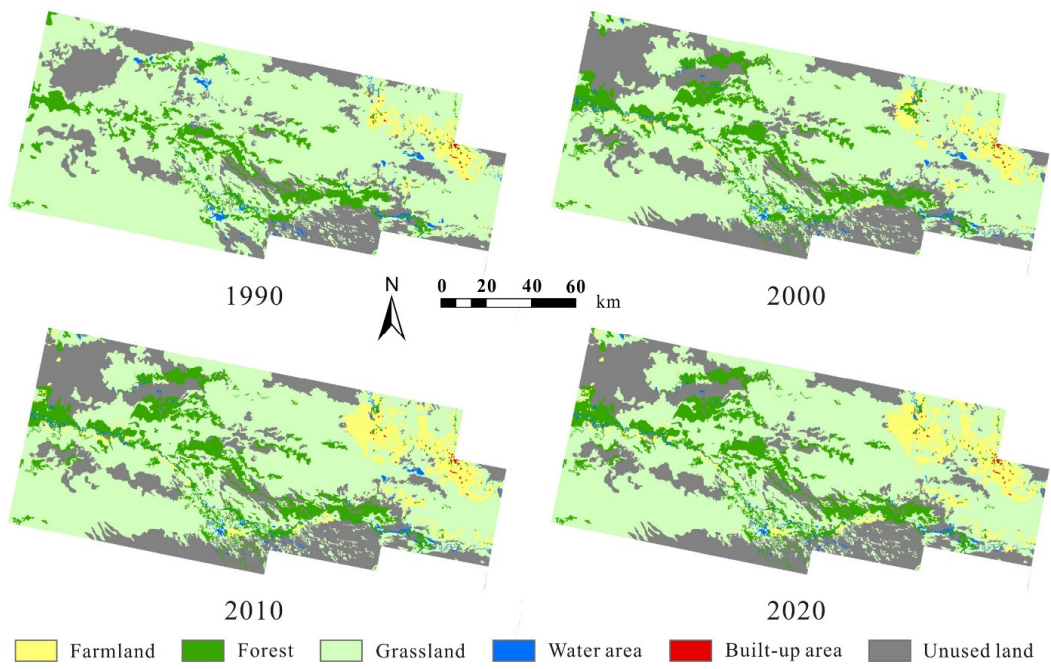
Figure 5. Land use and land cover maps in the middle reaches of the Tarim River.
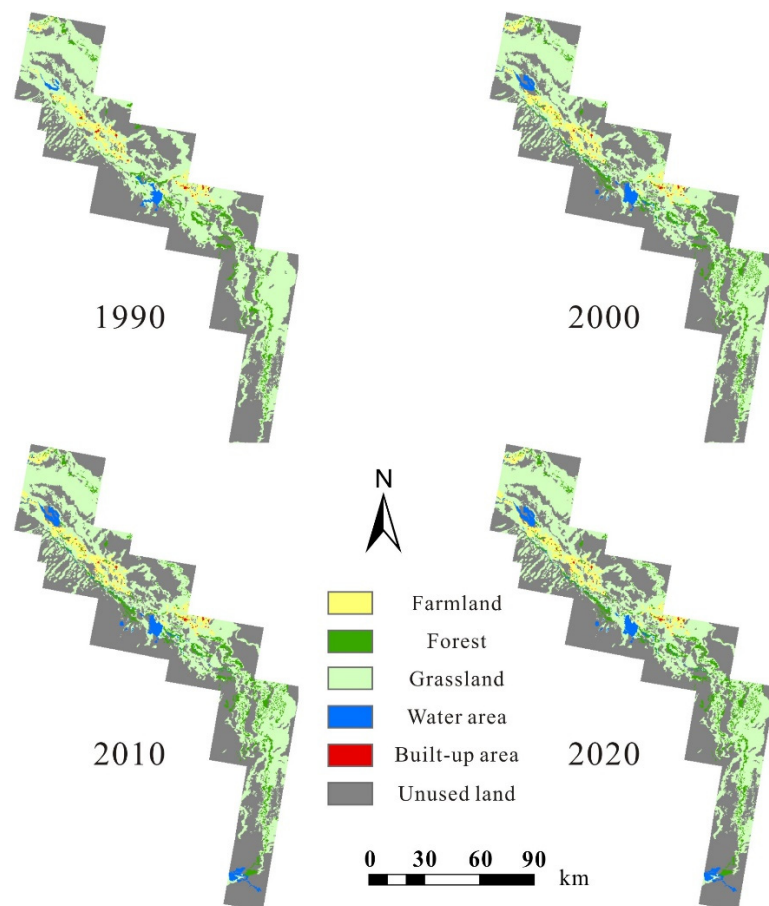

Figure 6. Land use and land cover maps in the lower reaches of the Tarim River.

4. Discussion and Policy Implications

Water resources play fundamental roles in arid and semi-arid areas. Although ecological water conveyance policies can restore biodiversity and vegetation in the lower reaches of rivers to a considerable extent, the upper and middle reaches may also suffer from some land use and environmental problems. Therefore, appropriate measures should be taken to carefully balance the benefits and risks of these man-made projects. First, local governments should develop a more reasonable water allocation plan for resolving the conflicts between upstream and downstream regions, especially when the headstreams (e.g., Bosten Lake) are at a lower water level. In a hopeful manner, the allocation of water resources should be as equitable as possible. Second, local governments should strictly control the annual growth rates of built-up areas and farmland (especially for water-intensive crops), which are the major consumers of underground and surface water. Although cotton is a highly profitable cash crop in Xinjiang, it is still necessary to balance its economic development and environmental conservation. The national "Returning Farmland to Forest and Grassland" and "Payments for Environmental Services" policies would be helpful in reducing land degradation, desertification, and other environmental issues. Third, drip irrigation methods should be widely promoted to replace traditional flood irrigation. The former is a new irrigation system that can distribute water directly onto the roots of crops and minimize evaporation, while the latter involves the flow of water over the ground and through the crops. This improvement could effectively save water in arid and semi-arid areas.

In summary, this study could provide practical policy implications for other similar inter-basin water conveyance attempts. One of the advantages of our analyses is that level-2 remote sensing classification results were adopted to better reflect the detailed LULC changes. For example, there are substantial differences between the ecological importance of lakes and reservoirs, even though they both belong to the "water area" category. Nevertheless, several aspects could still be improved in future experiments. For example, this study only considered the influence of ecological water conveyance projects on land use conditions. In future studies, we will take into account more relevant indicators (e.g., biological diversity and groundwater levels) to further investigate the influence of water conveyance. In addition, we will compare the Tarim River Basin with other regions that have also carried out water conveyance projects. We can explore whether the aforementioned effects are common phenomena.

5. Conclusions

This study found that the implementation of ecological water conveyance policies, which convey water resources in a direction from upstream to downstream, could exert notable influences on LULC changes in arid and semi-arid areas. The consideration of water conveyance routes made almost no difference to LULC modeling at first but could substantially improve the simulation accuracy after the application of water conveyance. While previous studies have mainly focused on positive outcomes, much less attention has been given to the influence of these policies on LULC conditions. To this end, our study found that water conveyance will more or less have unintended consequences on the LULC conditions in the upper and middle reaches of the study area (Tarim River region). For example, water and forest areas in the upper and middle reaches exhibited an obvious upward trend before the implementation of the ecological water conveyance project. Although these projects did improve environmental conditions in the lower reaches, some valuable natural resources in the upper and middle reaches slightly decreased in return, according to the detailed remote sensing classification data. With the Tarim River region being a primary objective of such large projects, this study contributes to a clear and comprehensive understanding of their influences on LULC conditions. These findings should draw the attention of decision makers to the unintended influence of water conveyance, and they could provide a valuable reference for environmental management and decisions in other similar arid and semi-arid areas.

References

1. Verburg, P.H.; Crossman, N.; Ellis, E.C.; Heinimann, A.; Hostert, P.; Mertz, O.; Nagendra, H.; Sikor, T.; Erb, K.-H.; Golubiewski, N.; et al. Land system science and sustainable development of the earth system: A global land project perspective. *Anthropocene* **2015**, *12*, 29–41. [CrossRef]
2. Cao, M.; Zhu, Y.; Quan, J.; Zhou, S.; Lü, G.; Chen, M.; Huang, M. Spatial Sequential Modeling and Predication of Global Land Use and Land Cover Changes by Integrating a Global Change Assessment Model and Cellular Automata. *Earth's Future* **2019**, *7*, 1102–1116. [CrossRef]
3. Marques-Carvalho, R.; Almeida, C.M.d.; Escobar-Silva, E.V.; Oliveira Alves, R.B.d.; Anjos Lacerda, C.S.d. Simulation and Prediction of Urban Land Use Change Considering Multiple Classes and Transitions by Means of Random Change Allocation Algorithms. *Remote Sens.* **2023**, *15*, 90. [CrossRef]
4. Guan, Q.; Shi, X.; Huang, M.; Lai, C. A hybrid parallel cellular automata model for urban growth simulation over GPU/CPU heterogeneous architectures. *Int. J. Geogr. Inf. Sci.* **2016**, *30*, 494–514. [CrossRef]
5. Li, H.; Peng, Y.; Li, M.; Zhuang, Y.; He, X.; Lin, J. Analyzing spatial patterns and influencing factors of different illegal land use types within ecological spaces: A case study of a fast-growing city. *J. Clean. Prod.* **2023**, *424*, 138883. [CrossRef]
6. Liu, X.; Huang, Y.; Xu, X.; Li, X.; Li, X.; Ciais, P.; Lin, P.; Gong, K.; Ziegler, A.D.; Chen, A.; et al. High-spatiotemporal-resolution mapping of global urban change from 1985 to 2015. *Nat. Sustain.* **2020**, *3*, 564–570. [CrossRef]
7. Gao, C.; Wang, J.; Wang, M.; Zhang, Y. Simulating Urban Agglomeration Expansion in Henan Province, China: An Analysis of Driving Mechanisms Using the FLUS Model with Considerations for Urban Interactions and Ecological Constraints. *Land* **2023**, *12*, 1189. [CrossRef]
8. Li, M.; Luo, H.; Qin, Z.; Tong, Y. Spatial-Temporal Simulation of Carbon Storage Based on Land Use in Yangtze River Delta under SSP-RCP Scenarios. *Land* **2023**, *12*, 399. [CrossRef]
9. Li, M.; Lin, J.; Ji, Z.; Chen, K.; Liu, J. Grid-Scale Poverty Assessment by Integrating High-Resolution Nighttime Light and Spatial Big Data—A Case Study in the Pearl River Delta. *Remote Sens.* **2023**, *15*, 4618. [CrossRef]
10. Lin, J.; Qiu, S.; Tan, X.; Zhuang, Y. Measuring the relationship between morphological spatial pattern of green space and urban heat island using machine learning methods. *Build. Environ.* **2023**, *228*, 109910. [CrossRef]
11. Zhong, J.; Jiao, L.; Droin, A.; Liu, J.; Lian, X.; Taubenböck, H. Greener cities cost more green: Examining the impacts of different urban expansion patterns on NPP. *Build. Environ.* **2023**, *228*, 109876. [CrossRef]
12. Yang, J.; Yang, Y.; Sun, D.; Jin, C.; Xiao, X. Influence of urban morphological characteristics on thermal environment. *Sustain. Cities Soc.* **2021**, *72*, 103045. [CrossRef]
13. Guan, X.; Li, J.; Yang, C.; Xing, W. Development Process, Quantitative Models, and Future Directions in Driving Analysis of Urban Expansion. *ISPRS Int. J. Geo-Inf.* **2023**, *12*, 174. [CrossRef]
14. He, C.; Gao, B.; Huang, Q.; Ma, Q.; Dou, Y. Environmental degradation in the urban areas of China: Evidence from multi-source remote sensing data. *Remote Sens. Environ.* **2017**, *193*, 65–75. [CrossRef]
15. Huang, Q.; Liu, Z.; He, C.; Gou, S.; Bai, Y.; Wang, Y.; Shen, M. The occupation of cropland by global urban expansion from 1992 to 2016 and its implications. *Environ. Res. Lett.* **2020**, *15*, 084037. [CrossRef]
16. Ke, X.; van Vliet, J.; Zhou, T.; Verburg, P.H.; Zheng, W.; Liu, X. Direct and indirect loss of natural habitat due to built-up area expansion: A model-based analysis for the city of Wuhan, China. *Land Use Policy* **2018**, *74*, 231–239. [CrossRef]
17. Yu, Y.; He, J.; Tang, W.; Li, C. Modeling Urban Collaborative Growth Dynamics Using a Multiscale Simulation Model for the Wuhan Urban Agglomeration Area, China. *ISPRS Int. J. Geo-Inf.* **2018**, *7*, 176. [CrossRef]
18. Wang, Q.; Liu, D.; Gao, F.; Zheng, X.; Shang, Y. A Partitioned and Heterogeneous Land-Use Simulation Model by Integrating CA and Markov Model. *Land* **2023**, *12*, 409. [CrossRef]

19. Li, S.; Zhuang, C.; Tan, Z.; Gao, F.; Lai, Z.; Wu, Z. Inferring the trip purposes and uncovering spatio-temporal activity patterns from dockless shared bike dataset in Shenzhen, China. *J. Transp. Geogr.* **2021**, *91*, 102974. [CrossRef]

20. McDonald, R.I.; Weber, K.; Padowski, J.; Flörke, M.; Schneider, C.; Green, P.A.; Gleeson, T.; Eckman, S.; Lehner, B.; Balk, D.; et al. Water on an urban planet: Urbanization and the reach of urban water infrastructure. *Glob. Environ. Chang.* **2014**, *27*, 96–105. [CrossRef]

21. Liao, J.; Tang, L.; Shao, G. Coupling Random Forest, Allometric Scaling, and Cellular Automata to Predict the Evolution of LULC under Various Shared Socioeconomic Pathways. *Remote Sens.* **2023**, *15*, 2142. [CrossRef]

22. Zuo, Y.; Zhang, L. Research on Local Ecosystem Cultural Services in the Jiangnan Water Network Rural Areas: A Case Study of the Ecological Green Integration Demonstration Zone in the Yangtze River Delta, China. *Land* **2023**, *12*, 1373. [CrossRef]

23. Zhou, Q.; Li, B.; Chen, Y. Remote Sensing Change Detection and Process Analysis of Long-Term Land Use Change and Human Impacts. *Ambio* **2011**, *40*, 807–818. [CrossRef] [PubMed]

24. Feng, Y.; Chen, S.; Tong, X.; Lei, Z.; Gao, C.; Wang, J. Modeling changes in China's 2000–2030 carbon stock caused by land use change. *J. Clean. Prod.* **2020**, *252*, 119659. [CrossRef]

25. Liu, Y.; He, Q.; Tan, R.; Liu, Y.; Yin, C. Modeling different urban growth patterns based on the evolution of urban form: A case study from Huangpi, Central China. *Appl. Geogr.* **2016**, *66*, 109–118. [CrossRef]

26. Li, F.; Li, Z.; Chen, H.; Chen, Z.; Li, M. An agent-based learning-embedded model (ABM-learning) for urban land use planning: A case study of residential land growth simulation in Shenzhen, China. *Land Use Policy* **2020**, *95*, 104620. [CrossRef]

27. Li, X.; Zhou, Y.; Gong, P. Diversity in global urban sprawl patterns revealed by Zipfian dynamics. *Remote Sens. Lett.* **2023**, *14*, 565–575. [CrossRef]

28. Shu, B.; Zhu, S.; Qu, Y.; Zhang, H.; Li, X.; Carsjens, G.J. Modelling multi-regional urban growth with multilevel logistic cellular automata. *Comput. Environ. Urban Syst.* **2020**, *80*, 101457. [CrossRef]

29. Long, Y.; Wu, K. Simulating Block-Level Urban Expansion for National Wide Cities. *Sustainability* **2017**, *9*, 879. [CrossRef]

30. Evans, J.M.; Calabria, J.; Borisova, T.; Boellstorf, D.E.; Sochacka, N.; Smolen, M.D.; Mahler, R.L.; Risse, L.M. Effects of local drought condition on public opinions about water supply and future climate change. *Clim. Chang.* **2015**, *132*, 193–207. [CrossRef]

31. Hammer, M.; Balfors, B.; Mörtberg, U.; Petersson, M.; Quin, A. Governance of Water Resources in the Phase of Change: A Case Study of the Implementation of the EU Water Framework Directive in Sweden. *Ambio* **2011**, *40*, 210–220. [CrossRef] [PubMed]

32. Destouni, G.; Jaramillo, F.; Prieto, C. Hydroclimatic shifts driven by human water use for food and energy production. *Nat. Clim. Chang.* **2013**, *3*, 213–217. [CrossRef]

33. Xu, H.; Ye, M.; Li, J. The water transfer effects on agricultural development in the lower Tarim River, Xinjiang of China. *Agric. Water Manag.* **2008**, *95*, 59–68. [CrossRef]

34. Zhang, X.; Chen, Y.; Li, W.; Yu, Y.; Sun, Z. Restoration of the lower reaches of the Tarim River in China. *Reg. Environ. Chang.* **2013**, *13*, 1021–1029. [CrossRef]

35. Smith, H.M.; Blackstock, K.L.; Wall, G.; Jeffrey, P. River basin management, development planning, and opportunities for debate around limits to growth. *J. Hydrol.* **2014**, *519*, 2624–2631. [CrossRef]

36. Chen, Y.; Chen, Y.; Xu, C.; Ye, Z.; Li, Z.; Zhu, C.; Ma, X. Effects of ecological water conveyance on groundwater dynamics and riparian vegetation in the lower reaches of Tarim River, China. *Hydrol. Process.* **2010**, *24*, 170–177. [CrossRef]

37. Ye, Z.; Chen, Y.; Li, W.; Yan, Y. Effect of the ecological water conveyance project on environment in the Lower Tarim River, Xinjiang, China. *Environ. Monit. Assess.* **2009**, *149*, 9–17. [CrossRef]

38. Chipman, J.W.; Shi, X.; Magilligan, F.J.; Chen, Y.; Li, B. Impacts of land cover change and water management practices on the Tarim and Konqi river systems, Xinjiang, China. *J. Appl. Remote Sens.* **2016**, *10*, 046020. [CrossRef]

39. Liu, J.; Zang, C.; Tian, S.; Liu, J.; Yang, H.; Jia, S.; You, L.; Liu, B.; Zhang, M. Water conservancy projects in China: Achievements, challenges and way forward. *Glob. Environ. Chang.* **2013**, *23*, 633–643. [CrossRef]

40. Bao, A.; Huang, Y.; Ma, Y.; Guo, H.; Wang, Y. Assessing the effect of EWDP on vegetation restoration by remote sensing in the lower reaches of Tarim River. *Ecol. Indic.* **2017**, *74*, 261–275. [CrossRef]

41. Zhang, S.; Ye, Z.; Chen, Y.; Xu, Y. Vegetation responses to an ecological water conveyance project in the lower reaches of the Heihe River basin. *Ecohydrology* **2017**, *10*, e1866. [CrossRef]

42. Armitage, D.; de Loë, R.C.; Morris, M.; Edwards, T.W.D.; Gerlak, A.K.; Hall, R.I.; Huitema, D.; Ison, R.; Livingstone, D.; MacDonald, G.; et al. Science–policy processes for transboundary water governance. *Ambio* **2015**, *44*, 353–366. [CrossRef]

43. Chen, Y.; Ye, Z.; Shen, Y. Desiccation of the Tarim River, Xinjiang, China, and mitigation strategy. *Quat. Int.* **2011**, *244*, 264–271. [CrossRef]

44. Xu, H.; Ye, M.; Song, Y.; Chen, Y. The Natural Vegetation Responses to the Groundwater Change Resulting from Ecological Water Conveyances to the Lower Tarim River. *Environ. Monit. Assess.* **2007**, *131*, 37–48. [CrossRef] [PubMed]

45. Li, W.; Hao, X.; Chen, Y.; Zhang, L.; Ma, X.; Zhou, H. Response of groundwater chemical characteristics to ecological water conveyance in the lower reaches of the Tarim River, Xinjiang, China. *Hydrol. Process.* **2010**, *24*, 187–195. [CrossRef]

46. Zhou, Q.; Li, B.; Kurban, A. Spatial pattern analysis of land cover change trajectories in Tarim Basin, northwest China. *Int. J. Remote Sens.* **2008**, *29*, 5495–5509. [CrossRef]

47. Akron, A.; Ghermandi, A.; Dayan, T.; Hershkovitz, Y. Interbasin water transfer for the rehabilitation of a transboundary Mediterranean stream: An economic analysis. *J. Environ. Manag.* **2017**, *202*, 276–286. [CrossRef]

48. Genereux, D.P.; Wood, S.J.; Pringle, C.M. Chemical tracing of interbasin groundwater transfer in the lowland rainforest of Costa Rica. *J. Hydrol.* **2002**, *258*, 163–178. [CrossRef]

49. Zhao, R.; Chen, Y.; Shi, P.; Zhang, L.; Pan, J.; Zhao, H. Land use and land cover change and driving mechanism in the arid inland river basin: A case study of Tarim River, Xinjiang, China. *Environ. Earth Sci.* **2013**, *68*, 591–604. [CrossRef]

50. Guo, Q.; Feng, Q.; Li, J. Environmental changes after ecological water conveyance in the lower reaches of Heihe River, northwest China. *Environ. Geol.* **2009**, *58*, 1387. [CrossRef]

51. Gohari, A.; Eslamian, S.; Mirchi, A.; Abedi-Koupaei, J.; Massah Bavani, A.; Madani, K. Water transfer as a solution to water shortage: A fix that can Backfire. *J. Hydrol.* **2013**, *491*, 23–39. [CrossRef]

52. Barnett, J.; Rogers, S.; Webber, M.; Finlayson, B.; Wang, M. Sustainability: Transfer project cannot meet China's water needs. *Nature* **2015**, *527*, 295. [CrossRef] [PubMed]

53. Mubako, S.; Nnko, H.J.; Peter, K.H.; Msongaleli, B. Evaluating historical and predicted long-term land use/land-cover change in Dodoma Urban District, Tanzania: 1992–2029. *Phys. Chem. Earth Parts A/B/C* **2022**, *128*, 103205. [CrossRef]

54. Hou, Y.; Chen, Y.; Li, Z.; Li, Y.; Sun, F.; Zhang, S.; Wang, C.; Feng, M. Land Use Dynamic Changes in an Arid Inland River Basin Based on Multi-Scenario Simulation. *Remote Sens.* **2022**, *14*, 2797. [CrossRef]

55. Mamitimin, Y.; Simayi, Z.; Mamat, A.; Maimaiti, B.; Ma, Y. FLUS Based Modeling of the Urban LULC in Arid and Semi-Arid Region of Northwest China: A Case Study of Urumqi City. *Sustainability* **2023**, *15*, 4912. [CrossRef]

56. Xie, L.; Wang, H.; Liu, S. The ecosystem service values simulation and driving force analysis based on land use/land cover: A case study in inland rivers in arid areas of the Aksu River Basin, China. *Ecol. Indic.* **2022**, *138*, 108828. [CrossRef]

57. Alqadhi, S.; Mallick, J.; Balha, A.; Bindajam, A.; Singh, C.K.; Hoa, P.V. Spatial and decadal prediction of land use/land cover using multi-layer perceptron-neural network (MLP-NN) algorithm for a semi-arid region of Asir, Saudi Arabia. *Earth Sci. Inform.* **2021**, *14*, 1547–1562. [CrossRef]

58. Hao, X.; Li, W. Impacts of ecological water conveyance on groundwater dynamics and vegetation recovery in the lower reaches of the Tarim River in northwest China. *Environ. Monit. Assess.* **2014**, *186*, 7605–7616. [CrossRef]

59. Chen, Y.; Li, W.; Liu, J.; Yang, Y. Effects of water conveyance embankments on riparian forest communities at the middle reaches of the Tarim River, Northwest China. *Ecohydrology* **2013**, *6*, 937–948. [CrossRef]

60. Tayyebi, A.; Pijanowski, B.C. Modeling multiple land use changes using ANN, CART and MARS: Comparing tradeoffs in goodness of fit and explanatory power of data mining tools. *Int. J. Appl. Earth Obs. Geoinf.* **2014**, *28*, 102–116. [CrossRef]

61. Li, X.; Chen, G.; Liu, X.; Liang, X.; Wang, S.; Chen, Y.; Pei, F.; Xu, X. A New Global Land-Use and Land-Cover Change Product at a 1-km Resolution for 2010 to 2100 Based on Human–Environment Interactions. *Ann. Am. Assoc. Geogr.* **2017**, *107*, 1040–1059. [CrossRef]

62. Li, S.; Lyu, D.; Liu, X.; Tan, Z.; Gao, F.; Huang, G.; Wu, Z. The varying patterns of rail transit ridership and their relationships with fine-scale built environment factors: Big data analytics from Guangzhou. *Cities* **2020**, *99*, 102580. [CrossRef]

63. Lin, J.; Li, X.; Wen, Y.; He, P. Modeling urban land-use changes using a landscape-driven patch-based cellular automaton (LP-CA). *Cities* **2023**, *132*, 103906. [CrossRef]

64. He, Q.; Zhou, J.; Tan, S.; Song, Y.; Zhang, L.; Mou, Y.; Wu, J. What is the developmental level of outlying expansion patches? A study of 275 Chinese cities using geographical big data. *Cities* **2020**, *105*, 102395. [CrossRef]

65. Lin, J.; Zhang, W.; Wen, Y.; Qiu, S. Evaluating the association between morphological characteristics of urban land and pluvial floods using machine learning methods. *Sustain. Cities Soc.* **2023**, *99*, 104891. [CrossRef]

66. Pontius, R.G.; Boersma, W.; Castella, J.C.; Clarke, K.; Nijs, T.D.; Dietzel, C.; Duan, Z.; Fotsing, E.; Goldstein, N.; Kok, K. Comparing the input, output, and validation maps for several models of land change. *Ann. Reg. Sci.* **2008**, *42*, 11–37.

67. Liu, X.; Liang, X.; Li, X.; Xu, X.; Ou, J.; Chen, Y.; Li, S.; Wang, S.; Pei, F. A future land use simulation model (FLUS) for simulating multiple land use scenarios by coupling human and natural effects. *Landsc. Urban Plan.* **2017**, *168*, 94–116. [CrossRef]

68. Liang, X.; Guan, Q.; Clarke, K.C.; Liu, S.; Wang, B.; Yao, Y. Understanding the drivers of sustainable land expansion using a patch-generating land use simulation (PLUS) model: A case study in Wuhan, China. *Comput. Environ. Urban Syst.* **2021**, *85*, 101569. [CrossRef]

69. Wu, H.; Luo, W.; Lin, A.; Hao, F.; Olteanu-Raimond, A.-M.; Liu, L.; Li, Y. SALT: A multifeature ensemble learning framework for mapping urban functional zones from VGI data and VHR images. *Comput. Environ. Urban Syst.* **2023**, *100*, 101921. [CrossRef]

70. Wang, H.; Zhang, B.; Xia, C.; He, S.; Zhang, W. Using a maximum entropy model to optimize the stochastic component of urban cellular automata models. *Int. J. Geogr. Inf. Sci.* **2020**, *34*, 924–946. [CrossRef]

71. Xu, Q.; Zhu, A.X.; Liu, J. Land-use change modeling with cellular automata using land natural evolution unit. *Catena* **2023**, *224*, 106998. [CrossRef]

72. He, J.; Li, C.; Yu, Y.; Liu, Y.; Huang, J. Measuring urban spatial interaction in Wuhan Urban Agglomeration, Central China: A spatially explicit approach. *Sustain. Cities Soc.* **2017**, *32*, 569–583. [CrossRef]

73. Lin, J.; He, P.; Yang, L.; He, X.; Lu, S.; Liu, D. Predicting future urban waterlogging-prone areas by coupling the maximum entropy and FLUS model. *Sustain. Cities Soc.* **2022**, *80*, 103812. [CrossRef]